Introduction

Radar system performance is fundamentally constrained by the optimality of the transmitted waveform. For modulated radar signals, the ability to resolve and distinguish targets in range is a result of the waveforms autocorrelation structure which is jointly determined by its time–bandwidth product and modulation structure. Consequently, waveform design is often formulated as the task of shaping the transmission signal to yield a ideal autocorrelation response, with particular emphasis on controlling the mainlobe width and sidelobe structure.

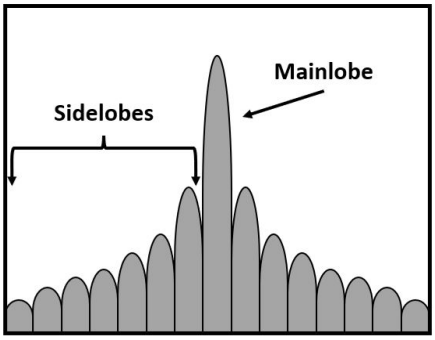

The time–bandwidth product, a system-dependent parameter, primarily governs the main-lobe width of the correlation response and thus directly determines the achievable range resolution. In contrast, the modulation structure, which is a design-dependent property, dictates the shape and magnitude of the sidelobes in the correlation function. Excessive sidelobe energy can mask weaker targets located near stronger reflections, leading to degraded detection and estimation performance [1]. Therefore, the design of radar waveforms must carefully balance resolution and sidelobe suppression to achieve a desirable correlation structure.

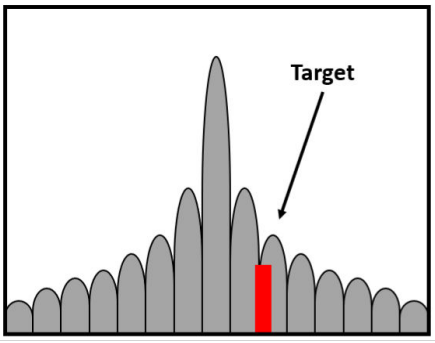

Problem Formulation:

The objective of the proposed waveform optimization framework is to minimize the autocorrelation sidelobes of a modulated radar waveform while maintaining a fixed time–bandwidth product. The objective function to be used is defined as

$$J = ||\mathbf{w}_{SL} \odot \mathbf{r}||_p^p$$

where $\mathbf{w}_{SL}$ is a binary mainlobe mask applied to the resulting autocorrelation structure $\mathbf{r}$. Therefore minimizing J directly minimizes the resulting correlation sidelobe levels. Specifically, the correlation response is computed as

$$\mathbf{r} = \mathbf{A}^H((\mathbf{A}\mathbf{s}) \odot (\mathbf{A}\mathbf{s})^*),$$

formed as the inverse Fourier transform of the waveforms power spectral density. Here, $\mathbf{s} \in \mathbb{C}^{Nx1}$ denotes the discrete complex waveform samples, $\mathbf{A}$ denotes the discrete Fourier transform operator, and $\mathbf{A}^H$ corresponds to its Hermitian (conjugate-inverse) transform. As stated, the binary weighting mask $\mathbf{w}_{SL}$ removes the contribution of the mainlobe region, ensuring that the optimization process focuses exclusively on sidelobe minimization. The p-norm provides a tunable measure of the sidelobe energy, with $p = 2$ corresponding to the average criterion and $p = \infty$ theoretically corresponding to the minimization of the maximum [2].

In addition to sidelobe suppression, the waveform must satisfy two physical constraints to ensure both hardware compatibility and spectral compliance. To minimize distortion and maintain efficient operation through the transmit amplifier, the waveform is required to exhibit a constant-envelope property, such that the magnitude of each complex sample has unity:

$$h(\mathbf{s}) = |\mathbf{s}|^2 - \mathbf{1} = \mathbf{0}.$$

This constraint preserves phase-only modulation and prevents nonlinear distortion introduced by amplitude variations in the amplifier. Furthermore, to satisfy spectral containment requirements imposed by the finite system bandwidth and FCC regulation, the waveforms frequency content must remain contained within a predescribed band. This is enforced through spectral mask $\mathbf{w}_F$, which limits the out-of-band spectral energy relative to the total signal power:

$$g(\mathbf{s}) = ||\mathbf{s}_F \odot (\mathbf{A}\mathbf{s})||_2^2 - \gamma||\mathbf{s}||_2^2.$$

The first term in the above inequality penalizes spectral energy in regions weighted by $\mathbf{w}_F$ while the second term scales the allowable leakage energy through the design parameter γ. Together, these constraints define a feasible design space of physically realizable, spectrally contained, and constant-envelope waveforms. The optimization problem is therefore formulated to achieve an optimal balance between autocorrelation performance and practical transmission constraints, fully defined below.

$$\begin{aligned} &\min_{\mathbf{s}} ||\mathbf{w}_{SL} \odot \mathbf{r}||_p^p \\ &\text{s.t } |\mathbf{s}|^2 - \mathbf{1} = \mathbf{0}, \\ &||\mathbf{w}_F \odot (\mathbf{A}\mathbf{s})||_2^2 - \gamma||s||_2^2 \leq 0 \end{aligned}$$

Convexity Analysis

To assess the convexity of the defined problem and motivate an appropriate solver, each term in the formulation must be analyzed individually before combining them into a cumulative objective. Starting with the definition of

$$\mathbf{r} = \mathbf{A}^H((\mathbf{As}) \odot (\mathbf{As})^*),$$

note that both $\mathbf{As}$ and $(\mathbf{As})^*$ represent linear and conjugate-linear transformations of $\mathbf{s}$; both individually preserving convexity. The hadamard product between the two, however, is bilinear in $\mathbf{s}$ (linear independently but not jointly) and therefore non-convex in general. For this special case where the same linear operator $\mathbf{A}$ appears in both terms, each row of the resulting element wise multiplication simplifies to

$$|\mathbf{As}|_k^2 = |\mathbf{a}_k^H \mathbf{s}|^2 = \mathbf{s}^H(\mathbf{a}_k \mathbf{a}_k^H)\mathbf{s},$$

which is convex quadratic since $\mathbf{a}_k \mathbf{a}_k^H \succcurlyeq 0$. Applying the inverse Fourier transform matrix $\mathbf{A}^H$ corresponds to a linear combination of these quadtratic terms

$$r_i = \sum_k A_{ki}^* \mathbf{a}_k \mathbf{s}^2,$$

in which convexity is preserved if and only if all coefficients of $\mathbf{A}^H$ are real and nonnegative. Being that $\mathbf{A}^H$ does not satisfy this requirement, $\mathbf{r}$ is non-convex. The application of the binary mainlobe mask can similarly be expressed as a linear mapping using the diagonal operator and therefore does not affect convexity; however, since convexity of $\mathbf{r}$ was already lost in the preceding operation, this transformation has no further effect on the solution space geometry apart from a uniform.

The equality constraint $|\mathbf{s}|^2 - \mathbf{1} = \mathbf{0}$ forces each entry to lie on the unit circle in $\mathbb{C}$ and therefore is non-convex. The inequality constraint, however, can be written in as a linear mapping using $\mathrm{Diag}(\mathbf{w}_F) = \mathbf{D}$ in place of the hadamard product and is alternately expressed as

$$|\mathbf{D(As)}|^2 - \gamma||s||_2 = (\mathbf{DAs})^H(\mathbf{DAs}) - \gamma \mathbf{s}^H \mathbf{Is} \leq 0.$$

and further simplified into a generalized inner-product form

$$(\mathbf{DAs})^H(\mathbf{DAs}) - \gamma \mathbf{s}^H \mathbf{Is} = \mathbf{s}^H(\mathbf{A}^H \mathbf{D}^H \mathbf{DA} - \gamma \mathbf{I})\mathbf{s} \leq 0.$$

Being that all terms within the paretheses are constant, γ is set such that $\mathbf{A}^H \mathbf{D}^H \mathbf{DA} - \gamma \mathbf{I}$ is indefinite and therefore solutions that satisfy the inequality constraint correspond to a nonconvex quadtraic solution space.

Proposed Routine

From the analysis performed in the previous section, the waveform design problem is highly non-convex, with non-convexity arising in both the objective function and the equality and inequality constraints. This structure rules out the use of standard convex optimization tools and motivates the adoption of a more robust nonlinear programming (NLP) framework. For this reason, the non-convex Augmented Lagrangian Method (ALM) was selected. Unlike classical Lagrange multiplier approaches—which can be unstable and provide no corrective force when constraints are violated—the augmented formulation incorporates quadratic penalty terms that regularize the subproblems, improve conditioning, and guiding iterates toward feasibility [4].

To formally introduce the augmented formulation, it is useful to begin with the classical Lagrangian framework from which ALM is derived. The method of Lagrange multipliers provides the foundational approach for solving

constrained nonlinear optimization problems by enforcing the Karush–Kuhn–Tucker (KKT) conditions [4, 5]. For equality constraints $h(\mathbf{x}) = \mathbf{0}$, the traditional Lagrangian is defined as

$$\mathscr{L}(\mathbf{x}, \boldsymbol{\lambda}) = f(\mathbf{x}) + \boldsymbol{\lambda}^T h(\mathbf{x}),$$

and feasible stationary points are obtained by simultaneously satisfying the gradient conditions $\nabla_{\mathbf{x}} \mathscr{L} = \mathbf{0}$ and the feasibility conditions $h(\mathbf{x}) = \mathbf{0}$. While this formulation provides intuitive theoretical analysis, it is poorly suited as a practical numerical method as the resulting system of nonlinear equations is often strongly ill-conditioned [4], requiring a separate nonlinear solver that is sensitive to initialization and typically converges only for simple problems. Moreover, the classical Lagrangian includes no mechanism that penalizes constraint violations. Points that are slightly infeasible produce almost no corrective force in the objective landscape, resulting in iterates wandering far from the constraint manifold [4, 7]. As a consequence, the traditional approach provides the right optimality conditions but lacks a stable, well-conditioned pathway for actually computing solutions.

The Augmented Lagrangian Method improves upon these issues by incorporating a quadratic penalty term into the Lagrangian [7, 8], yielding

$$\mathscr{L}(\mathbf{x}, \boldsymbol{\lambda}) = f(\mathbf{x}) + \boldsymbol{\lambda}^T h(\mathbf{x}) + \frac{\mu}{2} \|h(\mathbf{x})\|_2^2.$$

The additional term is active only when the constraints are violated, effectively creating a barrier that smoothly pushes the iterates toward feasibility. This penalty significantly improves conditioning of the subproblems [7, 8], making each unconstrained minimization step far more stable. Additionally, the dual variables become more well behaved as the algorithm incorporates the explicit update

$$\boldsymbol{\lambda}_{k+1} = \boldsymbol{\lambda}_k + \mu_k h(\mathbf{x}_k),$$

which allows the multipliers to converge reliably even in challenging problem landscapes [6]. Unlike pure penalty methods—which require $\mu \to \infty$ and thus produce strongly ill-conditioned subproblems—ALM achieves accurate constraint satisfaction using moderate penalty parameters, blending the strengths of multiplier methods and quadratic penalties without inheriting their weaknesses [3, 8].

Implementation

As established in the *Problem Formulation* section, the waveform design problem consists of minimizing the sidelobe energy subject to a constant-envelope equality constraint and a spectral-containment inequality constraint. For convenience, the formulation is rewritten below.

$$\begin{aligned} &\min_{\mathbf{s}} \; ||\mathbf{w}_{SL} \odot \mathbf{r}||_p^p \\ &\text{s.t} \;\; |\mathbf{s}|^2 - \mathbf{1} = \mathbf{0}, \\ &||\mathbf{w}_F \odot (\mathbf{A}\mathbf{s})||_2^2 - \gamma ||s||_2^2 \leq 0 \end{aligned}$$

To incorporate these constraints into a unified optimization framework, Lagrange multipliers $\lambda \in \mathbb{R}^N$ are introduced for the constant-envelope equality constraints, and a nonnegative multiplier $\mu \geq 0$ is associated with the spectral-mask inequality constraint. The corresponding standard Lagrangian is then

$$\mathscr{L}(\mathbf{s}, \boldsymbol{\lambda}, \mu) = f(\mathbf{s}) + \boldsymbol{\lambda}^T h(\mathbf{s}) + \mu g(\mathbf{s}),$$

where $f(\mathbf{s})$ denotes the sidelobe objective, $h(\mathbf{s})$ constant-envelope, and $g(\mathbf{s})$ is the spectral-leakage measure. To form the Augmented Lagrangian, quadratic penalty terms are added that stabilize the updates and improve constraint satisfaction. Specifically, the equality constraint is penalized by $\rho/2\|h(\mathbf{s})\|_2^2$, while the inequality constraint is penalized by $\eta/2[\max(0, g(\mathbf{s})]^2$, which activates only when the spectral leakage exceeds the allowable threshold.

Combinding the standard Lagrangian with these penalty terms yeilds

$$\mathscr{L}_{\rho,\eta}(\mathbf{s}, \boldsymbol{\lambda}, \mu) = ||\mathbf{w}_{SL} \odot \mathbf{r}||_p^p + \boldsymbol{\lambda}^T(|s|^2 - \mathbf{1}) + \frac{\rho}{2}\||s|^2 - \mathbf{1}\|_2^2 + \mu g(\mathbf{s}) + \frac{\eta}{2}[\max(0, g(\mathbf{s}))]^2.$$

To solve the now unconstrained augmented Lagrangian system, an iterative primal–dual algorithm is emplyed in which the waveform $\mathbf{s}$ is updated by minimizing the augmented Lagrangian with respect to $\mathbf{s}$ via gradient-descent, while the dual variables (λ, μ) are updated using gradient-ascent steps. This allows for the nonconvex objectiveand its constraints to all be handled within a unified gradient-based framework.

0. Gradient Derivations

As implied, the gradient of the objective and two constaints are required for the subsequent framework. Full gradient derivations can be found in the attached `GradientDerivations.pdf` document with the results for each component summarized below.

$$\nabla_{\mathbf{s}} J = 2\mathbf{A}^H\left[\mathbf{As} \odot \mathbf{A}\left(p|\mathbf{w}_{SL}|^p \odot |\mathbf{r}|^{p-2} \odot \mathbf{r}\right)\right]$$

$$\nabla_{\mathbf{s}}[\boldsymbol{\lambda}^T h(\mathbf{s})] = 2\boldsymbol{\lambda} \odot \mathbf{s}$$

$$\nabla_{\mathbf{s}} g(\mathbf{s}) = 2\mathbf{A}^H(|\mathbf{w}_F|^2 \odot (\mathbf{As})) - 2\gamma\mathbf{s}$$

$$\nabla_{\mathbf{s}}\left[\frac{\rho}{2}||h(\mathbf{s})||_2^2\right] = 2p(|\mathbf{s}|^2 - \mathbf{1}) \odot \mathbf{s}$$

$$\nabla_{\mathbf{s}}\left[\mu g(\mathbf{s}) + \frac{\eta}{2}(\max(0, g(\mathbf{s})))^2\right] = \begin{cases} \mu\nabla_{\mathbf{s}} g(\mathbf{s}) & \text{for } g(\mathbf{s}) \le 0, \\ (\mu + \eta g(\mathbf{s}))\nabla_{\mathbf{s}} g(\mathbf{s}) & \text{for } g(\mathbf{s}) > 0. \end{cases}$$

1. Primal Update

At iteration k, the primal update solves $\mathbf{s}_{k+1} = \arg\min_{\mathbf{s}} \mathscr{L}_{\rho,\eta}(\mathbf{s}, \boldsymbol{\lambda}_k, \mu_k)$ which is performed using the gradient-descent step defined below where α_k is the step size set statically here for simplicity.

$$\mathbf{s}_{k+1} = \mathbf{s}_k - \alpha_k \nabla_{\mathbf{s}} \mathscr{L}_{\rho,\eta}(\mathbf{s}, \boldsymbol{\lambda}_k, \mu_k)$$

2. Dual Update

Once the primal variable $\mathbf{s}_{k+1}$ is computed, the dual variables λ_{k+1} and μ_{k+1} are subsequently updated. For equality constraint multipliers, the gradient ascent step is performed as

$$\lambda_{k+1} = \lambda_k + \rho h(\mathbf{s}_{k+1}).$$

The inequality constraint mutliplier is likewise performed as

$$\mu_{k+1} = \max\left(0, \mu_k + \eta g(\mathbf{s}_{k+1})\right)$$

where the $\max$ operator ensures that $\mu \geq 0$.

3. Stopping Conditions

The iterative algorithm is terminated when both feasibility and convergence criteria are satisfied. First, the primal constraints must be approximately met, meaning that the constant-envelope condition falls below a prescribed tolerance, ϵ_h, and the spectral-mask inequality likewise satisfies $g(\mathbf{s}) \leq \epsilon_g$. Second, the optimization must exhibit convergence in the sense that the change in the sidelobe objective between successive iterations becomes negligible and the gradient norm of the augmented Lagrangian satisfies $||\nabla_{\mathbf{s}} \mathscr{L}_{\rho,\eta}||_2 \leq \epsilon_\nabla$. When both the constraint residuals and gradient-based convergence metrics meet their respective thresholds, the algorithm is declared to have converged to a feasible stationary point.

Convergence and Optimality

The full implementation of the Augmented Lagrangian Method used is provided in the accompanying MATLAB function `generateOptimizedLFM.m` along with the supporting scripts that contain closed-form gradient expressions for both the objective and constraint functions. The implementation follows the formulation developed in the preceding sections and incorporates statically selected tuning parameters to streamline development and enable controlled analysis of algorithm behavior.

To establish a baseline for comparison, the optimization procedure is initialized using a linear frequency modulated (LFM) waveform. The LFM serves as a natural starting point due to its widespread use in sensing applications and its desirable properties with a perfectly flat envelope, modest spectral containment, and peak sidelobe levels of approximately –13 dB in its autocorrelation response. These characteristics provide a feasible and physically meaningful initialization from which the algorithm can further refine.

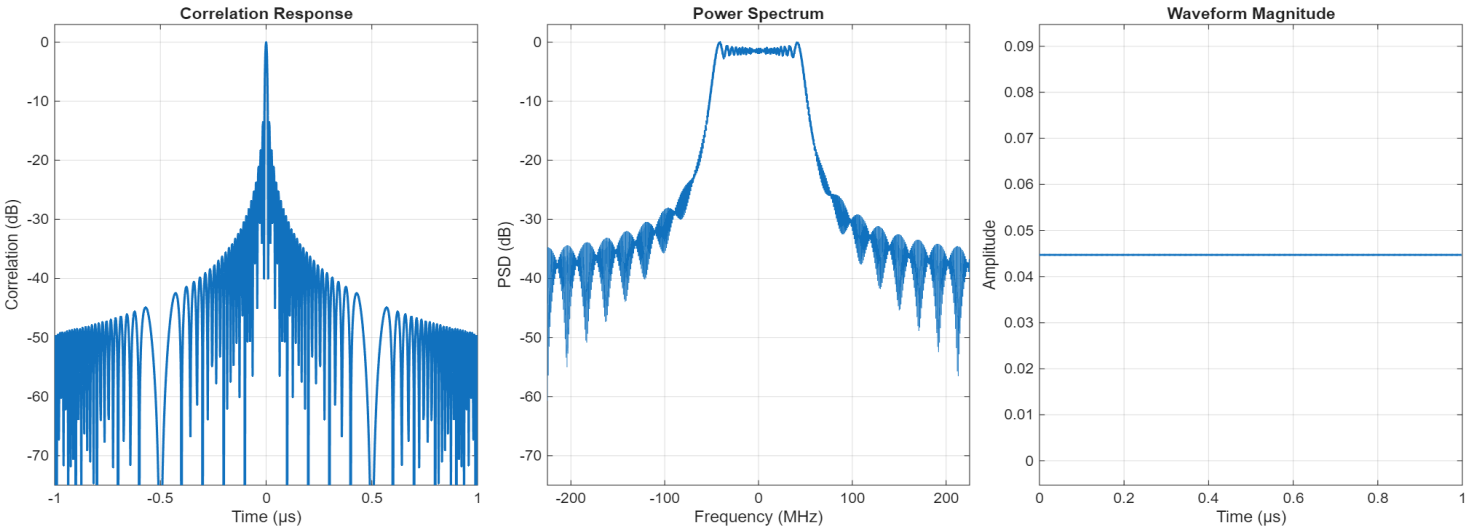

After executing the augmented Lagrangian routine for 200 iterations, the algorithm produces an optimized waveform that exhibits significant performance improvements. The resulting design achieves –22 dB peak sidelobe levels, enhanced spectral containment, and a slight but controlled amount of envelope ripple relative to the initial LFM. The magnitude of this ripple is directly influenced by the equality-constraint penalty parameter ρ, which determines how strongly deviations from the constant-envelope condition are penalized. Because the penalty parameters are held fixed in this implementation, the algorithm is sensitive to their selection and can struggle to enforce the equality constraint more strictly without compromising numerical stability.

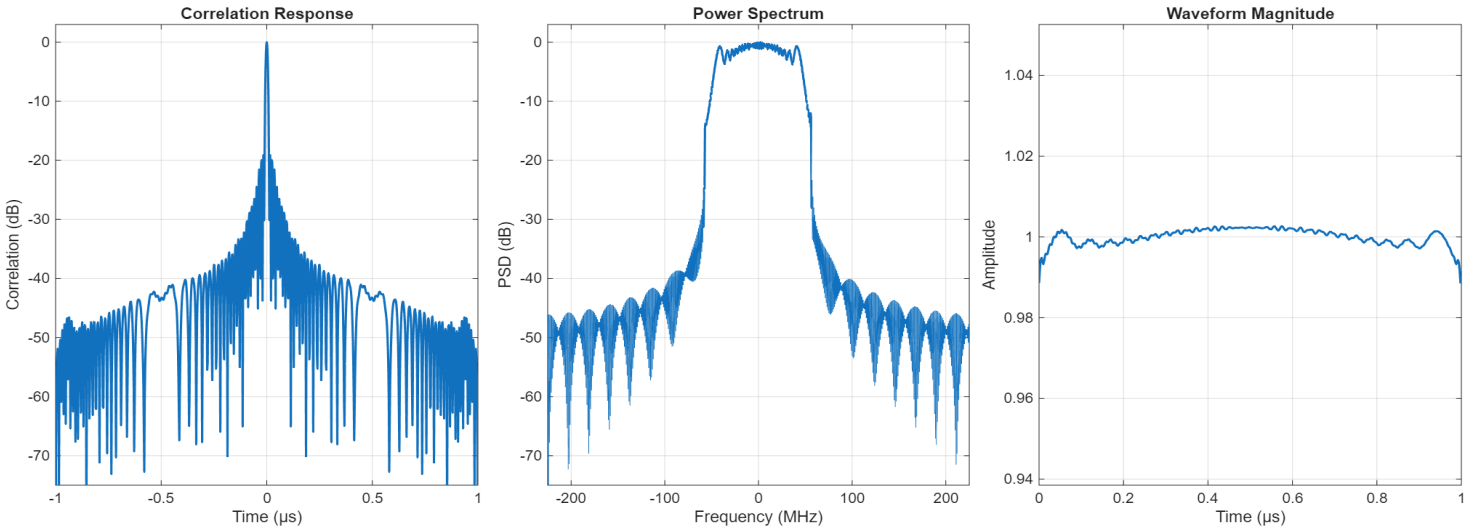

The behavior of the ALM implementation can be assessed through the evolution of four key quantities: (1) the sidelobe objective value, (2) the equality ‐ constraint residual, (3) the inequality ‐ constraint residual, and (4) the gradient norm of the augmented Lagrangian. Together, these measures provide evidence for convergence toward a feasible stationary point in the constrained nonconvex solution space.

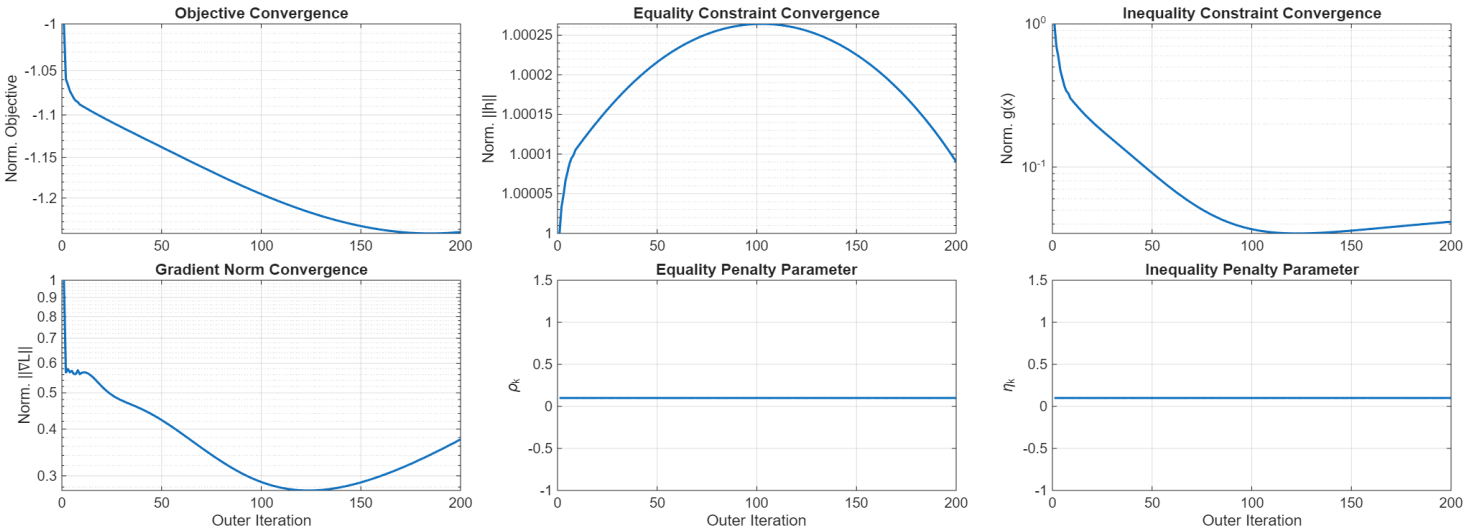

The top-left plot of the figure shown above demonstrates a monotonic decrease of the sidelobe objective over the 200 iterations. This behavior is consistent with the expected effect of the augmented Lagrangian penalty terms: as constraint violations diminish, descent steps are allowed to target improvements in sidelobe level. The curve also gradually flattens, indicating diminishing returns and suggesting that the algorithm has neared a stationary point where further progress becomes limited by the constraint structure.

The top-middle plot shows the residual of the constant-envelope constraint over the primal iterations. The residual initially increases—an expected effect when the algorithm prioritizes objective reduction or inequality feasibility—but subsequently decreases once the envelope penalty term and dual variables have adapted. This behavior demonstrates the adaptive balancing inherent to ALM: early iterations permit moderate feasibility violations to escape poor regions of the landscape, while later iterations progressively enforce tighter satisfaction as the multiplier and penalty parameters stabilize. Although the final envelope ripple is small but nonzero, the trend shows that the algorithm is effectively steering the waveform back toward the constraint manifold.

Similarly, the top-right plot shows the spectral-containment constraint residual which decreases smoothly and reaches near-zero. This indicates that ALM is successfully regulating spectral leakage and enforcing the mask once the multipliers have stabilized. Importantly, the inequality multiplier remains nonnegative and increases only when violations are present—behavior consistent with the complementary slackness structure of KKT conditions.

Across all metrics, the algorithm exhibits the hallmark features of a stable augmented Lagrangian method: smooth and consistent objective descent, decreasing constraint violations, stable multipliers, and a diminishing gradient norm which translate to physically meaningful waveform improvements. While the final solution is not globally optimal due to nonconvexity, the convergence trends indicate that the method has reached a near-feasible, locally optimal stationary point.

Conclusions

The waveform design problem examined in this work seeked to minimize autocorrelation sidelobes while simultaneously satisfying two physically motivated constraints. Being that both the objective and constraints

were proven to be strongly non-convex, the Augmented Lagrangian Method was adopted due to its ability to stably enforce constraints through quadratic penalties while maintaining the flexibility needed to navigate complex optimization landscapes. The ALM framework, supported by analytically derived gradients, was implemented using a primal–dual iterative routine and initialized with a conventional LFM waveform. The algorithm successfully produced a waveform with significantly reduced peak sidelobe levels, improved spectral containment, and modest envelope ripple. These results demonstrate that the augmented Lagrangian approach provides a effective pathway for designing practical, high-performance radar waveforms under realistic physical constraints.

Citations

[1] M. A. Richards, Fundamentals of Radar Signal Processing, 3rd ed. New York, NY, USA: McGraw-Hill, 2022.

[2] J. Owen, D. Felton, P. Asuzu, V. Amendolare, and S. Blunt, "Hybrid Random FM Waveforms for Enhanced Range Sidelobe Performance," in Proc. IEEE Int. Radar Conf., Rennes, France, 2024.

[3] S. Zhao, Z. Frangella, and M. Udell, "NysADMM: faster composite convex optimization via low-rank approximation," in Proc. 39th Int. Conf. on Machine Learning (ICML), Baltimore, MD, USA, 2022.

[4] D. P. Bertsekas, Nonlinear Programming, 2nd ed. Belmont, MA, USA: Athena Scientific, 1999.

[5] S. Boyd and L. Vandenberghe, Convex Optimization. Cambridge, U.K.: Cambridge Univ. Press, 2004.

[6] R. T. Rockafellar, "The multiplier method of Hestenes and Powell applied to convex programming," J. Optimization Theory and Applications, vol. 12, no. 6, pp. 555–562, 1973.

[7] M. J. D. Powell, "A method for nonlinear constraints in minimization problems," in Optimization, R. Fletcher, Ed. New York, NY, USA: Academic Press, 1969, pp. 283–298.

[8] J. Nocedal and S. J. Wright, Numerical Optimization, 2nd ed. New York, NY, USA: Springer, 2006.